

<https://doi.org/10.15407/ujpe65.3.236>

R.M. RUDENKO,¹ O.O. VOITSIHOVSKA,¹ V.V. VOITOVYCH,¹ M.M. KRAS'KO,¹
A.G. KOLOSUYUK,¹ V.YU. POVARCHUK,¹ M.P. RUDENKO,² L.M. KNOROZOK²

¹ Institute of Physics, Nat. Acad. of Sci. of Ukraine

(46, Prosp. Nauky, Kyiv 03028, Ukraine; e-mail: rudenko.romann@gmail.com)

² Mykola Gogol State University of Nizhyn

(2 Grafts'ka Str., Nizhyn 16600, Ukraine)

FORMATION OF NANOCRYSTALLINE SILICON IN TIN-DOPED AMORPHOUS SILICON FILMS

The process of crystalline silicon phase formation in tin-doped amorphous silicon (a-SiSn) films has been studied. The inclusions of metallic tin are shown to play a key role in the crystallization of researched a-SiSn specimens with Sn contents of 1–10 at% at temperatures of 300–500 °C. The crystallization process can conditionally be divided into two stages. At the first stage, the formation of metallic tin inclusions occurs in the bulk of as-precipitated films owing to the diffusion of tin atoms in the amorphous silicon matrix. At the second stage, the formation of the nanocrystalline phase of silicon occurs as a result of the motion of silicon atoms from the amorphous phase to the crystalline one through the formed metallic tin inclusions. The presence of the latter ensures the formation of silicon crystallites at a much lower temperature than the solid-phase recrystallization temperature (about 750 °C). A possibility for a relation to exist between the sizes of growing silicon nanocrystallites and metallic tin inclusions favoring the formation of nanocrystallites has been analyzed.

Keywords: nanocrystalline silicon, metal-induced crystallization, tin.

1. Introduction

Trends in the development of modern electronics require the application of functional elements about a few nanometers in size. Therefore, the technologies aimed at the formation of semiconductor nanostructures are actively developed and the physical properties of the latter are intensively studied. Since silicon is the most wide-spread semiconductor material, considerable attention of scientists is focused on the study of nanocrystalline silicon (nc-Si), the properties of which are substantially different from those of the crystalline (c-Si) and amorphous (a-Si) materials.

Nanocrystalline silicon extends the scope of applications of silicon-based materials. For example, the radiative recombination in nc-Si, unlike that in c-Si, can be realized without the mandatory participation of phonons, as it occurs in direct-band semiconduc-

tors [1]. Therefore, nanocrystalline silicon in the silicon suboxide (SiO_x) matrix is used as a basis for the creation of light-emitting devices in the visible and near IR spectral intervals [2–4]. At the same time, amorphous-nanocrystalline silicon films serve as a basis for producing the highly efficient multilayer solar cells and so forth [5, 6].

The physical properties of thin silicon and silicon suboxide films depend to a large extent on the ratio between the numbers of particles of the amorphous and nanocrystalline phases, as well as on the size and concentration of silicon nanocrystals [2, 3, 7–9]. Nanocrystalline inclusions are also believed to partially relieve mechanical stresses in the amorphous matrix, thus resulting in a possibility to form a less strained network with a fewer number of weak bonds, which is more robust to degradation under the action of external factors [6, 7]. By monitoring the content ratio between the amorphous and crystalline phases in such films, it is possible to control their optical and electrical properties. Therefore, it is important to understand the mechanism of nanocrystalline silicon formation.

© R.M. RUDENKO, O.O. VOITSIHOVSKA,
V.V. VOITOVYCH, M.M. KRAS'KO,
A.G. KOLOSUYUK, V.YU. POVARCHUK,
M.P. RUDENKO, L.M. KNOROZOK, 2020

There are plenty of methods aimed at the nc-Si formation. Among them, methods based on the application of metals [10–13] should be distinguished. It is known that metals can significantly lower the crystallization temperature of amorphous silicon and accelerate this process. In recent years, the main attention of researchers has been focused on the study of the metal-induced crystallization in structures obtained by the layer-by-layer deposition of a metal and amorphous silicon [11]. Owing to thermal treatments, the metal and silicon layers exchange their places, and silicon simultaneously crystallizes. Many works were devoted to the study of mechanisms and conditions of microcrystalline silicon formation in such double-layer structures. However, the issues concerning the formation of silicon nanocrystals up to 10 nm in size as a result of the metal-induced crystallization have been studied rather poorly. In particular, as a rule, only the presence of silicon crystals several tens of nanometers in dimensions was reported without making any analysis of the preconditions of their formation (see, e.g., works [14, 15]).

It is known that even the application of the same metal may lead to the formation of nanocrystalline silicon in some cases and microcrystalline silicon in the others. For example, we showed earlier that the crystallization temperature in the amorphous silicon [7–9] and silicon suboxide [2] films that were tin-doped during their precipitation becomes lower, and the formation of nc-Si with crystallite sizes up to 10 nm takes place in them. The authors of work [14] reported on the formation of nanocrystalline silicon (<10 nm) in films obtained by simultaneously evaporating silicon and aluminium. Crystallites close in size can also be formed in specimens of amorphous silicon implanted with tin ions [15]. At the same time, it was shown in works [10–12, 16] that microcrystalline silicon (0.1–100 μm) is formed at the layer-by-layer precipitation of silicon and tin (or aluminium or other metals). Thus, the metal-induced crystallization of amorphous silicon can result in the formation of either nanocrystalline silicon (with crystallite sizes less than 10 nm) or microcrystalline silicon (with crystallite sizes exceeding 10 nm). The issue of which factor is crucial for silicon crystallites smaller than 10 nm in dimensions to be formed in the case of metal-induced crystallization still remains poorly examined. The understanding of relevant processes is of great practical importance, which de-

termines the challenging character of corresponding researches.

Among various metals that are suitable for performing the metal-induced silicon crystallization, tin should be put at the first place. First, unlike other metals, tin is an isovalent impurity to silicon. Second, tin is characterized by a low eutectic temperature of the silicon-tin alloy, which allows silicon crystallites to be obtained at rather low temperatures. Third, tin has a low solubility in crystalline silicon, which makes it possible to produce a crystalline material with lower contamination level in comparison with other metal impurities [17].

Therefore, the aim of this work was to study the peculiarities of the nanocrystalline silicon formation in amorphous films obtained by simultaneously precipitating silicon and tin.

2. Experimental Part

Experimental specimens of tin-doped amorphous silicon (a-SiSn) were obtained by thermally evaporating the powders of tin (the PO-1 grade, a purity grade of 99.1%, a grain size of 40–45 μm) and silicon (silicon KEF-4.5) in vacuum. The tin content in the researched specimens was 0, 1, 4, 10, and 15 at%. The films were precipitated onto silicon and quartz substrates at a temperature of 300 °C. The film thickness was 300–800 nm. The impurity content in the studied films was monitored using the Auger electron spectroscopy method on an Auger microprobe JAMP-9500F.

In order to change the phase composition in precipitated films, the latter were subjected to the isochronous annealing for 20 min in the argon atmosphere within the temperature interval from 300 to 750 °C with an increment of 50 °C. The phase composition of the films was studied by analyzing their Raman spectra. A detailed description of the method can be found in our previous works [8, 9]. The Raman spectra were registered at room temperature on a Jobin Yvon T-64000 spectrometer using the excitation radiation of an Ar⁺ laser with a wavelength of 488 nm. The average sizes of silicon crystallites and the fraction of the crystalline phase were estimated by resolving the Raman spectra into bands corresponding to the amorphous and crystalline phases in the framework of the spatial phonon confinement model [18–20]. The detailed information concerning

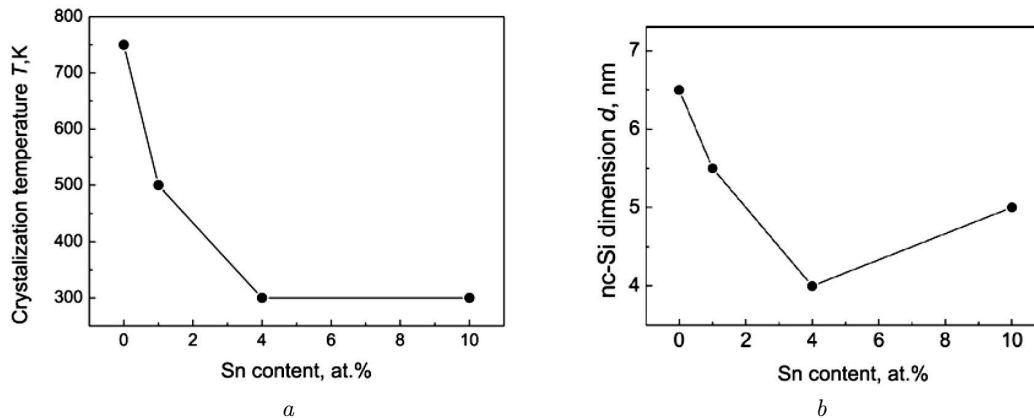


Fig. 1. Dependences of the crystallization temperature (a) and the size of silicon nanocrystals at the crystallization temperature (b) on the tin content in a-SiSn specimens

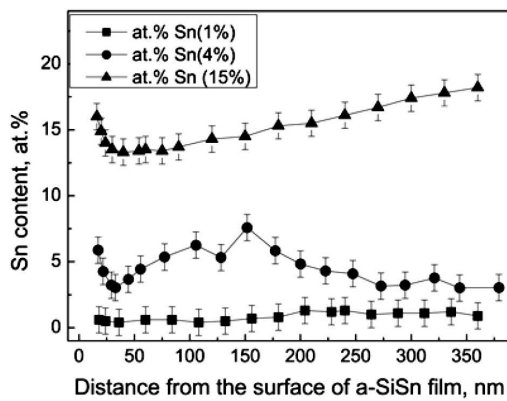


Fig. 2. Distribution profiles of the Sn impurity across a-SiSn films with various Sn contents

the method of producing the a-SiSn films, their impurity composition, and structural and optical characteristics can be found in works [7–9].

3. Experimental Results and Their Discussion

3.1. Experimental results

In Fig. 1, the dependences of the crystallization temperature (panel a) and the size of silicon nanocrystals at the crystallization temperature (panel b) on the tin content in a film within an interval of 0–10 at% are shown. One can see that the crystallization temperature of the a-SiSn specimens depends on the tin content and, for doped specimens, is lower than the crystallization temperature of pure (undoped) amorphous silicon (750 °C). For the specimens with a tin content

of 1 at%, the crystallization of the amorphous silicon phase occurred after their annealing at 500 °C. At the same time, in the specimens containing 4 and 10 at% of Sn, the crystalline phase was present immediately after the precipitation at 300 °C. The sizes of silicon crystallites in the specimens did not exceed 10 nm. In other words, tin has a significant effect on the formation of nanocrystalline silicon in the a-SiSn specimens at temperatures of 300–500 °C. The analysis of Raman spectra showed that the fraction of the crystalline phase after the crystallization amounted to 60–80% of the volume of examined a-SiSn films with the Sn content ranging from 0 to 10 at%.

Figure 2 demonstrates the tin impurity distribution over the film thickness for the specimens with Sn contents of 1, 4, and 15 at%. The exhibited profiles were obtained with the help of the reactive ion etching and Auger electron spectroscopy methods. The etching rate was about 15 nm/min. One can see that tin was almost uniformly distributed over the film volume. Taking into account that, immediately after the precipitation, the tin-free specimen and the specimen with 1 at% of Sn did not contain the crystalline silicon phase (Fig. 1), we will assume hereafter that Si and Sn atoms were uniformly distributed over the film volume, when the films were being precipitated and, thus, formed an amorphous structure of a-SiSn films.

The tin content in the experimental specimens was 1 at% or higher, i.e. higher than the limit of the tin solubility in crystalline silicon [17]. Therefore, it is very probable that metal clusters should be formed in the film bulk. According to the results of works

[11, 13, 21, 22], those clusters play a key role in a reduction of the crystallization temperature of the a-Si matrix in “amorphous silicon–metal” systems. Since the temperatures of the film precipitation and heat treatment were higher than the tin melting temperature (231.9°C [17]), tin clusters were probably formed in the liquid state.

3.2. Tin-induced lowering of the crystallization temperature of amorphous silicon

It is doubtful that the interaction of silicon and metal atoms at relatively low temperatures (close to the eutectic one) occurs without a weakening of the bonds between silicon atoms, because the covalent Si–Si bond is very strong (the corresponding binding energy is about 2 eV [23]). One of the possible explanations why the bonds between silicon atoms become weaker in the presence of metal atoms is the “screening model” proposed by S. Hiraki [24]. According to it, free electrons in metallic tin screen the Coulomb interaction forces that act between neighbor silicon atoms. As a result, the band gap becomes narrower, and the near-interface silicon region from 2 to 4 monolayers in thickness transits into the intrinsic metallic state [24].

The mixing of the near-interface silicon layer in the metallic state with metallic tin at low temperatures can be explained analogously to the mixing of metals. The most important factor at the metal mixing under low temperatures can be the cohesive (group) mechanism, which differs significantly from the mixing mechanism for covalent semiconductors [24]. The cohesive energy of a metal is mainly determined by the concentration of its free mobile electrons (electron gas). As long as the electron concentration does not increase, there are no electron-induced restrictions on the simultaneous motions of metal ions, which is required for the mixing to take place [24]. Therefore, the near-interface silicon layer that contacts with metallic tin, owing to the penetration of tin electrons into it, transits into an intrinsic metallic state. As a result, it will easily mix with metallic tin at relatively low temperatures, which provides the interaction of tin clusters with surrounding silicon.

In our specimens fabricated by simultaneously evaporating Si and Sn, the process of silicon–tin mixing most likely occurred similarly to the mixing of

amorphous silicon with aluminium in layered structures [10, 25]. As a rule, the activation energy of the diffusion of impurity atoms in metallic tin does not exceed that of the tin self-diffusion (1.1 eV [26]). At the same time, the activation energy of the diffusion of silicon atoms in liquid tin is even lower and equals about 0.2 eV [27]. It is easy to see that the indicated values are much lower than the activation energies of the Sn diffusion in c-Si (4–5 eV [28]) and a-Si (1.7 eV [29] or 1.3 eV [30]), and Si diffusion in c-Si (3–4 eV [31, 32]) and a-Si (2.8–4.4 eV [33, 34]). They are also lower than the activation energy of the recrystallization in amorphous silicon (3–4 eV [21, 33, 35]). Therefore, it is evident that if metallic tin is in contact with amorphous silicon, the penetration of silicon atoms into the metal is the most advantageous energetically. As a result, we arrive at the conclusion that a Si–Sn alloy will be formed in the bulk of researched films, because the tin clusters will dissolve the surrounding amorphous silicon matrix.

In the general case, the driving force of the structural ordering in amorphous silicon is the difference μ^E between the chemical potentials of silicon atoms in the amorphous, μ^{a-Si} , and crystalline, μ^{c-Si} , states [11],

$$\mu^E = \mu^{a-Si} - \mu^{c-Si} > 0. \quad (1)$$

Therefore, according to the equilibrium condition, μ^{a-Si} and μ^{c-Si} must correspond to the chemical potential of Si atoms in the Si–Sn alloy, which is in equilibrium with both disordered and crystalline silicon. According to the ideal solution model, the chemical potential of silicon atoms in the Si–Sn solution, μ^{Si} , depends on the silicon concentration X^{Si} ,

$$\mu^{Si} = \mu_0 + RT \ln X^{Si}, \quad (2)$$

where μ_0 is the chemical potential of silicon, R the universal gas constant, and T the absolute temperature.

The difference between the chemical potentials of Si atoms that are in equilibrium with the amorphous ($\mu^{Si} = \mu^{Sn/a-Si}$) and crystalline ($\mu^{Si} = \mu^{Sn/c-Si}$) structures leads to the difference between the corresponding equilibrium Sn concentrations in the disordered ($X^{Sn/a-Si}$) and crystalline ($X^{Sn/c-Si}$) silicon phases. Their ratio equals

$$\frac{X^{Sn/a-Si}}{X^{Sn/c-Si}} = \exp\left(\frac{\mu^E}{RT}\right) > 1. \quad (3)$$

This means that the solubility of silicon from the disordered phase is higher than the solubility of silicon from the ordered phase. This solubility difference is responsible for the transport of silicon atoms from the amorphous phase to the crystalline one through metallic tin, similarly to a-Si in the layered a-Si/Al structures [11, 21]. At the concentration $X^{\text{Sn}} < X^{\text{Sn/a-Si}}$, i.e. when $\mu^{\text{Sn}} < \mu^{\text{Sn/a-Si}}$, amorphous silicon will dissolve in the Si–Sn alloy. Accordingly, the chemical potential of amorphous silicon will decrease until the maximum solubility $X^{\text{Sn/a-Si}}$ is achieved. On the other hand, this solution is supersaturated with respect to crystalline silicon ($X^{\text{Sn}} > X^{\text{Sn/c-Si}}$, i.e. $\mu^{\text{Sn}} > \mu^{\text{Sn/c-Si}}$). Therefore, the silicon atoms leave the Si–Sn alloy and form a crystalline phase. In other words, during the growth of the crystalline silicon phase, there is a certain concentration X^{Sn} of silicon in the solution that is lower than the solubility limit of amorphous silicon in the Si–Sn alloy ($X^{\text{Sn/a-Si}}$) and simultaneously higher than the solubility limit of amorphous silicon in the crystalline phase ($X^{\text{Sn/c-Si}}$), i.e. $X^{\text{Sn/c-Si}} < X^{\text{Sn}} < X^{\text{Sn/a-Si}}$. Owing to the presence of metallic tin, silicon crystallizes, which is accompanied by a reduction of the chemical potential of Si atoms.

The processes described above explain well why the presence of metallic tin inclusions leads to a reduction of the crystallization temperature in the studied specimens. Tin clusters can dissolve silicon atoms from the amorphous matrix. When the silicon concentration in the solution reaches the solubility limit for the amorphous phase, the formed Si–Sn alloy turns out supersaturated with respect to the crystalline phase. Therefore, crystalline silicon precipitates.

3.3. Tin effect on the formation of nanocrystalline silicon

Now, let us try to elucidate which factors are crucial for the formation of silicon crystallites about a few nanometers in size in a-SiSn films. As was mentioned in Introduction, even the same metal can induce the formation of both nanocrystalline and microcrystalline silicon phases [10–12, 14–16]. Perhaps, this occurs, because different technologies are applied to the specimen fabrication. As a result, metal inclusions with different sizes are formed, and amorphous silicon contacts with them. In particular, at the layer-by-layer precipitation, the size of metal in-

clusions should most probably be larger, although it depends on the layer thickness. At the same time, at the ion implantation with metal or at the simultaneous precipitation of silicon and the metal, metal inclusions with relatively small sizes are formed in the a-Si matrix.

It is reasonable to assume that there may exist a relation between the size of silicon crystallites that are being formed and the size of tin clusters in which the amorphous phase dissolves. In other words, the size of silicon crystallites that are being formed is proportional to the size of metal inclusions that are participating in the formation of those crystallites.

Let us suppose that silicon nanocrystals are formed in the studied a-SiSn films, and let those nanocrystals consist of the same amount of Si atoms from a-Si that can be simultaneously dissolved in one metallic tin cluster, i.e. the actual value corresponds to the maximum solubility of Si atoms at the given temperature. According to this assumption, the larger the size of tin clusters, the larger the size of silicon crystallites formed in the film bulk. Let us also suppose that the metallic tin clusters that are formed in the film bulk have the same size, and every of those clusters can dissolve such a number of Si atoms from the amorphous matrix that is sufficient for the formation of silicon nanocrystals with dimensions equal to those experimentally determined in works [8, 9] (see Fig. 1). It is clear that these assumptions are idealized, because the real peculiarities in the formation of silicon crystallites in the presence of a metal are much more complicated, so that this process may depend on a large number of external conditions, including the temperature. However, such an idealization will allow us to draw some conclusions.

Let us assume that two processes take place simultaneously: some silicon atoms are quitting tin to form crystallites, whereas some others from the surrounding amorphous matrix are becoming dissolved in tin. If the temperature is constant, this process continues as long as the tin cluster is in contact with amorphous silicon. The authors of works [29, 36] considered metal clusters to be mobile in the amorphous matrix and, when moving, to leave a crystalline trace behind themselves. As a result of the motion of metallic inclusions, the amorphous matrix crystallizes. When the whole available surrounding amorphous matrix becomes crystallized, the process terminates because the concentration gradient

resulting from the difference between the solubility of silicon from the amorphous and crystalline matrices disappears.

In order to check the correctness of the assumption made above, let us use it as a basis to analyze the experimental results presented in this paper and in works [8, 9]. Let us firstly evaluate how many times the solubility of amorphous silicon in tin is higher than that of crystalline silicon. A system in which pure tin is in contact with a-Si is not in the thermal equilibrium. The supersaturated solution of silicon in tin is formed owing to the difference between the Gibbs energies for the metastable amorphous and stable crystalline silicon phases. This difference, the excess Gibbs energy μ_G^E , can be written in the form

$$\mu_G^E = \mu_G^{a-Si} - \mu_G^{c-Si} = h^E - Ts^E, \quad (4)$$

where μ_G^{a-Si} and μ_G^{c-Si} are the molar Gibbs energies for the amorphous and crystalline silicon phases, respectively; and $h^E = 11.9$ kJ/mol and $s^E = 1.66$ J/(mol · K) are the molar excess enthalpy and entropy, respectively [11, 33].

On the other hand, the excess Gibbs energy is related to the activity a by the equality [11]

$$\mu_G^E = RT \ln a, \quad (5)$$

where R is the universal gas constant, and T the absolute temperature. Therefore, in our case, taking Eq. (3) into account, the activity a characterizes how much the solubility of silicon from the amorphous phase is higher than the solubility of silicon from the crystalline one. Basing on the data concerning the temperature dependence of the excess Gibbs energy in amorphous silicon with respect to crystalline one, which can be found in work [37], we obtain that the activity coefficient for amorphous silicon is about 7.8 at a temperature of 300 °C and about 4.2 at 500 °C. Accordingly, the solubility of amorphous silicon at the indicated temperatures will be proportionally higher than that of crystalline silicon.

3.3.1. Dimensions of tin clusters in a-SiSn with Sn contents of 4 and 10 at%

As is shown in Fig. 1, in the bulk of as-precipitated a-SiSn films with Sn contents of 4 and 10 at%, there are silicon crystallites with an average size of about 4–5 nm, which corresponds to about 2500 Si

atoms. Taking into account that the solubility of silicon in tin equals 0.036 at% at a temperature of 300 °C (this value was calculated by interpolating the data of work [17]) and the activity $a \approx 7.8$ at this temperature, the solubility of amorphous silicon in tin is about 0.28 at%. Accordingly, a tin droplet capable of dissolving 2500 Si atoms has to be composed of about 10^6 Sn atoms, which corresponds to a transverse size of about 30–40 nm for a spherical tin droplet. According to the tin content in the indicated films, the distance between the centers of neighbor metal clusters with transverse sizes of 30–40 nm should be equal to about 75–80 nm on average, which corresponds to a tin inclusion concentration of about 2×10^{15} cm⁻³. The calculated values are almost identical to the size and concentration of tin clusters determined in work [38] by analyzing the TEM and HR TEM images of Si_{0.95}Sn_{0.05} films. This coincidence confirms the correctness of our assumption.

It should also be noted that, in the as-precipitated specimens with a tin content of 10 at%, the dimensions of nc-Si equaled 5 nm (Fig. 1), which was slightly larger than the dimensions of nc-Si in a-SiSn with an Sn content of 4 at%. Probably this tendency takes place owing to the circumstance that, in the films with the higher tin content, larger metallic inclusions can be formed, which also testifies to the correctness of our assumption.

Let us now determine the diffusion coefficient of tin in the researched a-SiSn films. As was evaluated above, the distance between the centers of neighbor tin clusters was about 80 nm, i.e. the diffusion sphere radius was about 40 nm. On the other hand, since the radii of tin clusters were approximately equal to 20 nm, the radius of the diffusion sphere equaled $20 \text{ nm} + \sqrt{Dt}$, where D is the diffusion coefficient of Sn in the film, and t the diffusion time. Let us take $t \approx 1000$ s. This is the total time required to precipitate the film on the substrate at 300 °C (from 100 to 200 s) and to gradually cool it down to a temperature of 200–250 °C (from 800 to 900 s). Lower temperatures were not taken into consideration, because, in this case, the solubility of Si in Sn becomes lower and the diffusion of Sn in Si slower by orders of magnitude [17, 28, 39].

Our mathematical calculations showed that the diffusion coefficient of tin in the amorphous structure of an a-SiSn film at $T = 300$ °C equals $D = 4 \times 10^{-15}$ cm²/s. The obtained value is much larger

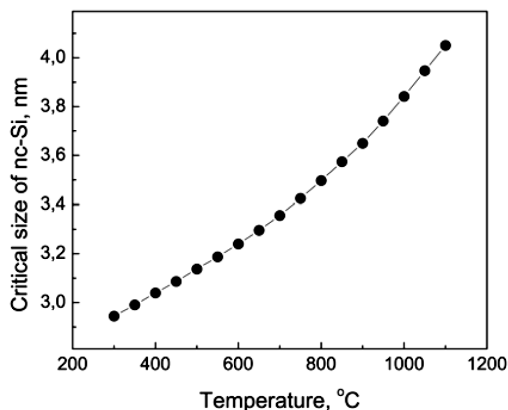


Fig. 3. Theoretical dependence of the critical size of silicon nanocrystals in a-Si on the temperature

than the value of the tin diffusion coefficient in crystalline silicon (in c-Si, the diffusion coefficient of Sn reaches $D = 5 \times 10^{-15} \text{ cm}^2/\text{s}$ only at $T = 1100 \text{ }^\circ\text{C}$ [28, 39], but it practically coincides with the value of the tin diffusion coefficient in amorphous hydrogenated silicon films a-Si:H, $D = 2.8 \times 10^{-15} \text{ cm}^2/\text{s}$ at $T = 300 \text{ }^\circ\text{C}$ [30]). Hence, the value of the tin diffusion coefficient in the amorphous silicon matrix, which was obtained theoretically in the framework of our assumption, is close to experimental data obtained in the works of other researchers. The coincidence of theoretical and experimental results testifies to the validity of our assumption about a correlation between the size of silicon nanocrystals and the size of tin clusters in the examined a-SiSn films.

Since the diffusion coefficient of tin in crystalline silicon is several orders of magnitude lower than that in amorphous silicon, it is the motion of Sn atoms in a-Si that allows the formation of metallic tin clusters in the researched a-SiSn films to take place. This conclusion is in good agreement with the activation energy Sn in a-Si, which was discussed above.

3.3.2. Dimensions of tin clusters in a-SiSn with Sn content of 1 at%

Let us now consider a-SiSn films with a tin content of about 1 at%. As is shown in Fig. 1, there was no crystalline phase in those films immediately after their precipitation. The nc-Si phase was only observed after the annealing at $500 \text{ }^\circ\text{C}$. In view of the above-calculated diffusion coefficient of tin in the studied films, we obtain that tin clusters with maxi-

imum transverse dimensions of about 10–15 nm and a distance between them of about 50 nm (or the corresponding concentration of metallic tin clusters equal to about $5 \times 10^{-15} \text{ cm}^{-3}$) can be formed in specimens with a tin content of about 1 at% during the time $t \approx 1000 \text{ s}$. Every tin cluster with those sizes can dissolve about 150 Si atoms in itself, which corresponds to a diameter of about 1.5–2 nm for a spherical silicon nanocrystal. The absence of bands associated with the crystalline phase in such specimens in their Raman spectra registered immediately after the precipitation [8, 9] can be explained by the inability of this method to detect rather small volumes of the crystalline phase. On the other hand, the obtained crystallite dimensions could be smaller than the critical ones at the given temperature. So, after the formation, they should immediately transit back into the amorphous state.

Let us evaluate the critical dimensions of silicon crystallites in the examined temperature interval. It is known that the critical radius of the nucleus can be calculated using the following expression [40]:

$$R_c = \frac{2\gamma_{ac}Q}{\mu^E}, \quad (6)$$

where γ_{ac} is the difference between the surface free energies of the amorphous, γ_a , and crystalline, γ_c , silicon phases (according to work [41], $\gamma_{ac} = 600 \text{ mJ/m}^2$), μ^E is the difference between the chemical potentials of silicon atoms in the amorphous and crystalline phases, and $Q = 12.1 \text{ cm}^3/\text{mol}$ is the molar volume of silicon. Using the value for the Gibbs free energy in the amorphous silicon phase with respect to the crystalline one, which is given in work [37], we obtain a theoretical dependence of the critical dimensions of silicon crystallites in a-Si on the temperature (Fig. 3). This dependence agrees well with the results obtained earlier in our works [7–9]. The dimensions of silicon nanocrystals observed in those works were larger than the critical ones within the whole temperature interval of the thermal treatment, 300–1100 °C.

As one can see from Fig. 3, the critical size of nc-Si nuclei at $T = 300 \text{ }^\circ\text{C}$ is about 3 nm. Therefore, silicon crystallites about 1.5–2 nm in size that were formed in the a-SiSn films with a tin content of about 1 at% immediately after the film precipitation turned out unstable and transited into the amorphous phase. This

scenario explains the absence of maxima corresponding to the crystalline phase of silicon in the Raman spectra registered for the a-SiSn specimens with an Sn content of about 1 at% immediately after their precipitation.

If the annealing temperature is increased to $T = 500$ °C, the solubility of c-Si in metallic Sn clusters grows to 0.14 at% (this value was obtained by interpolating the data from work [17]), and the activity of the amorphous silicon phase decreases to $a \approx 4.2$. But on the whole, the solubility limit of Si atoms (from the amorphous phase) in tin will increase to 0.56 at%, which is approximately twice as large as the corresponding value at a temperature of 300 °C, namely, 0.29 at%. Let us suppose that the tin clusters enlarge their sizes only in the course of the film precipitation, whereas a further heat treatment at temperatures above 300 °C does not lead to their growth. Then, after the annealing at 500 °C, the size of tin clusters will remain unchanged (about 10–15 nm), and the size of silicon crystallites will increase to 2–2.5 nm owing to a growth of the tin solubility. This value is also smaller than the critical dimensions of nc-Si at a temperature of 500 °C (Fig. 3). Therefore, the assumption that the size of tin clusters remains unchanged during their heat treatment is wrong.

Let us try to evaluate the sizes of tin clusters at an annealing temperature of 500 °C, proceeding from the average size of silicon crystallites that was determined experimentally ($d \approx 5.5$ nm, see Fig. 1). In this case, we obtain that the size of tin clusters has to equal about 35 nm, and the average distance between them to about 140 nm (which corresponds to a concentration of about 4×10^{14} cm⁻³). Hence, on the basis of the assumption that the dimensions of tin and silicon nanocrystals are interrelated, it follows that, after the annealing at 500 °C, the size of metallic tin clusters should increase from 10–15 nm to 35 nm in order to provide the possibility of the formation of nanocrystalline silicon with dimensions that exceed the critical ones. It should be noted that the growth of metallic tin clusters without their motion is improbable. Therefore, it is most likely that the metallic tin clusters move rather easily in the amorphous silicon matrix, because the growth of their sizes from 10–15 nm to 35 nm within a time interval of 600 s is possible.

For silicon nanocrystallites to be formed, the tin clusters must reach such dimensions, when they are capable of forming nc-Si nuclei with sizes larger than

the critical ones. Therefore, it becomes clear that the crystalline phase is absent in the a-SiSn specimens with an Sn content of about 1 at% immediately after their precipitation at 300 °C. It is so, because the total time of the film growing and cooling is not enough for the appearance of tin clusters with sizes sufficient to form stable silicon crystallites whose sizes are larger than the critical ones. Only after a further heat treatment, the tin clusters reach the required dimensions, and the crystalline phase of silicon is formed.

As was said above, the formed tin clusters will dissolve amorphous silicon. Afterward, this silicon will be removed from the solution in the form of crystallites. Thus, the crystallization process can be considered as a motion of silicon atoms from the amorphous to the crystalline phase through the tin clusters. Then the flux density J of Si atoms looks like [10]

$$J = cv, \quad (7)$$

where v is the velocity of the Si atom motion through tin clusters, and $c = 5 \times 10^{22}$ cm⁻³ is the concentration of silicon atoms.

3.3.3. Front velocity of nc-Si crystallization in a-SiSn

The difference between the concentrations of silicon in tin that is in equilibrium with either the amorphous, c_{a-Si} , or the crystalline, c_{c-Si} , phases is responsible for the motion of Si atoms from the a-Si phase to the c-Si one. Assuming that we deal with the case of one-dimensional diffusion, the first Fick's law can be written in the form

$$J = -D \frac{\partial c}{\partial x} \approx -D \frac{c_{a-Si} - c_{c-Si}}{d_{Sn}}, \quad (8)$$

where d_{Sn} is the transverse size of a tin cluster, and D is the diffusion coefficient of silicon in tin. Since the issue of the silicon diffusion in metallic tin has not been studied sufficiently well, we will assume that the diffusion coefficient of silicon in tin is equal to the tin self-diffusion coefficient at 300 °C, i.e. $D = 3 \times 10^{-5}$ cm²/s [42].

After relevant calculations, we obtain that, in the researched a-SiSn films, the velocity of Si atoms in tin clusters should be equal to $v \sim 10^{-2}$ cm/s. This value is much larger than the growth velocity of the crystalline phase at the thermally induced crystallization of amorphous silicon, namely, $v \sim (1 \div 10) \times$

$\times 10^{-10}$ cm/s at a temperature of 400–500 °C [25, 35]. However, it is comparable with the velocity of a crystallization front, when tin-doped silicon films are annealed at a temperature of 450 °C ($v \sim 10^{-4}$ cm/s, [15]). Such a high crystallization front velocity results from the fact that tin is in the liquid state at temperatures of 300–500 °C, so that the transport of Si atoms through it from the amorphous to the crystalline matrix is very fast.

At temperatures higher than the melting point of a metal, a similar picture is observed for other “amorphous silicon–metal” systems as well. For example, in work [36], it was reported that crystallization in silicon doped with In atoms occurred more than 10^4 times faster than the fastest solid phase epitaxy of silicon, and the process of specimen crystallization did not exceed 10 s. In the case where the diffusion occurs through a metal in the solid state, the crystallization front velocity will be much lower in accordance with the magnitude of the diffusion coefficient of silicon in a metal. In particular, for the aluminium-induced crystallization at temperatures of 400–500 °C, the crystallization front velocity $v \sim 10^{-8} \div 10^{-7}$ cm/s [10, 43].

The crystallization front velocity $v \sim 10^{-4} \div 10^{-2}$ cm/s will result in the crystallization of researched specimens within time intervals of an order of several tens of seconds or shorter. This interval is much shorter than the time of the tin cluster formation that was taken into consideration ($t \sim 1000$ s). This means that the time required for the crystallization of a-SiSn specimens is mainly determined by the time of the metallic tin cluster formation, i.e. it is limited by the time of the tin diffusion in amorphous silicon. Similar conclusions were drawn in work [29], when comparing the activation energies of the metal-induced crystallization and tin diffusion in a-Si.

Therefore, the crystallization process in the examined a-SiSn films with Sn contents of 1–10 at% can be divided into two stages. The first stage consists in the formation of tin clusters during the process of film cooling after the film precipitation or during a further heat treatment. The second stage includes the dissolution of silicon atoms from the amorphous matrix in tin clusters followed by the subsequent removal of those silicon atoms from the alloy in the form of a crystalline phase. The duration of the first stage is much longer than that of the second stage. The duration of the first stage is determined by the diffu-

sion of tin atoms in amorphous silicon and can last for about 1000 s at temperatures of 300–500 °C. The duration of the second stage most likely does not exceed a few tens of seconds, because it is determined by a rather high velocity of the crystallization front motion, which is governed, in turn, by the diffusion of silicon atoms through a molten tin droplet.

The analysis made above testifies that our assumption about the existence of a relation between the sizes of silicon crystallites that are being formed and the sizes of metallic tin inclusions favoring the formation of the crystalline silicon phase is in good agreement with our experimental results and with the results obtained by other researchers. Therefore, we may argue that metallic clusters play a crucial role in the metal-induced crystallization not only by reducing the crystallization temperature of the amorphous matrix, but also by substantially affecting the size of the crystals that are being formed. The influence of metallic tin on the formation of nanoscale silicon crystals in the researched films is most probably a result of the same physical processes that are responsible for the influence of nanoscale metallic clusters on the formation of silicon nanowires in the “vapor–liquid–solid”, “solid–liquid–solid”, and other scenarios [13]. The conclusion about the proportionality between the size of forming silicon crystallites and the size of metal inclusions favoring the crystallite formation has a large practical importance, because it points out a possible direction for the development of a technology aimed at the formation of nanocrystalline silicon with predetermined crystallite sizes.

4. Conclusions

The results obtained in this work allow the following conclusions to be drawn.

1. Metallic tin clusters play a major role in the processes of nanocrystalline silicon formation in the studied a-SiSn specimens with Sn contents of 1–10 at% at temperatures of 300–500 °C.
2. The process of nanocrystalline silicon formation can be divided into two stages. The first stage includes the formation of metallic tin clusters in the course of the precipitation and a further heat treatment. This stage is long-lasting, being determined by the diffusion of tin atoms in amorphous silicon. It can last for about 1000 s. The second stage includes the dissolution of the surrounding amorphous silicon ma-

trix in metallic tin clusters and the removal of silicon atoms from the melt in the form of nanocrystallites. This stage is short-term, being governed by the diffusion of silicon atoms from the amorphous silicon matrix to the crystalline one through metallic tin clusters. The duration of this stage does not exceed a few tens of seconds.

3. Our analysis of experimental results testifies that there is a relation between the sizes of silicon crystallites that are being formed and the sizes of metallic tin clusters favoring the crystallite formation. The proportionality between the crystallite size in the formed nc-Si and the size of metallic inclusions can be of large practical importance, because it points out a possible method of nanocrystalline silicon formation with predetermined crystallite sizes.

1. D. Kovalev, H. Heckler, G. Polisski, J. Diener, F.Koch. Optical properties of silicon nanocrystals. *Opt. Mater.* **17**, 35 (2001).
2. V.V. Voitovych, R.M. Rudenko, A.G. Kolosiuk, M.M. Kras'ko, V.O. Juhimchuk, M.V. Voitovych, S.S. Ponomarov, A.M. Kraitchinskii, V.Yu. Povarchuk, V.A. Makara. Effect of tin on the processes of silicon-nanocrystal formation in amorphous SiO_x thin-film matrices. *Semiconductors* **48**, 73 (2014).
3. V.V. Voitovych, R.M. Rudenko, V.O. Yuchymchuk, M.V. Voitovych, M.M. Kras'ko, A.G. Kolosiuk, V.Yu. Povarchuk, I.M. Khachevich, M.P. Rudenko. Effect of tin on structural transformations in the thin-film silicon suboxide matrix, *Ukr. J. Phys.* **61**, 980 (2016).
4. V. Švrček, A. Slaoui, J.-C. Muller. Silicon nanocrystals as light converter for solar cells. *Thin Solid Films* **451–452**, 384 (2004).
5. A. Kherodia, A.K. Panchal. Analysis of thickness-depedent optical parameters of a-Si:H/nc-Si:H multilayer thin films. *Mater. Renew. Sustain. Energy* **6**, 23 (2017).
6. A. Shan, E. Vallat-Shauvain, P. Torres, J. Meier, U. Kroll, C. Hof, C. Droz, M. Goerlitzer, N. Wyrsh, M. Vanechek. Intrinsic microcrystalline silicon (μ c-Si:H) deposited by VHF-GD (very high frequency-glow discharge): A new material for photovoltaics and optoelectronics. *Mater. Sci. Eng.* **69–70**, 219 (2000).
7. V.V. Voitovych, V.B. Neimash, N.N. Kras'ko, A.G. Kolosiuk, V.Yu. Povarchuk, R.M. Rudenko, V.A. Makara, R.V. Petrunya, V.O. Juhimchuk, V.V. Strelchuk. The effect of Sn impurity on the optical and structural properties of thin silicon films, *Semiconductors* **45**, 1281 (2010).
8. R.M. Rudenko, V.V. Voitovych, M.M. Kras'ko, A.G. Kolosyuk, A.M. Kraichynskiy, V.O. Yukhymchuk, V.A. Makara. Influence of high temperature annealing on the structure and the intrinsic absorption edge of thin-film silicon doped with tin. *Ukr. J. Phys.* **58**, 769 (2013).
9. R.M. Rudenko, M.M. Kras'ko, V.V. Voitovych, A.G. Kolosyuk, V.YU. Povarchuk, A.M. Kraichynskiy, V.O. Yukhymchuk, V.YA. Bratus', M.V. Voitovych, I.A. Zaloilo. Behavior of hydrogen during crystallization of thin silicon films doped with tin. *Ukr. J. Phys.* **58**, 1165 (2013).
10. T.J. Konno, R. Sinclair. Crystallization of silicon in aluminium/amorphous-silicon multilayers, *Phil. Mag. B* **66**, 749 (1992).
11. O. Nast, S.R. Wenham. Elucidation of the layer exchange mechanism in the formation of polycrystalline silicon by aluminium-induced crystallization. *J. Appl. Phys.* **88**, 124 (2000).
12. M. Jeon, C. Jeong, K. Kamisako. Tin induced crystallisation of hydrogenated amorphous silicon thin films. *Mater. Sci. Technol.* **26**, 875 (2010).
13. A. Sarikov. Metal induced crystallization mechanism of the metal catalyzed growth of silicon wire-like crystals. *Appl. Phys. Lett.* **99**, 143102 (2011).
14. Jae-Hyun Shim, Nam-Hee Cho. Formation of nanocrystallites in the nc-Si films by co-sputtering aluminium and silicon. *Solid State Phenom.* **124–126**, 495 (2007).
15. Fuyu Lin, Miltiadis. Crystallization of tin-implanted amorphous silicon thin films. *Mat. Res. Soc. Symp. Proc.* **279**, 553 (1993).
16. Jong-Hyeok Park, M. Kurosawa, N. Kawabata, M. Miyao, T. Sadoh. Au-induced low-temperature ($\sim 250^\circ\text{C}$) crystallization of Si on insulator through layer-exchange process, *Electrochem. Sol.-St. Lett.* **14**, H232 (2011).
17. R.W. Olesinski, G.J. Abbaschian. The Si-Sn (silicon-tin) system. *Bull. Alloy Phase Diagr.* **5**, 273 (1984).
18. P. Mishra, K.P. Jain. First- and second-order Raman scattering in nanocrystalline silicon. *Phys. Rev. B* **64**, 073304 (2001).
19. H. Campbell, P.M. Fauchet. The effects of microcrystal size and shape on the one phonon Raman spectra of crystalline semiconductors, *Solid State Commun.* **58**, 739 (1986).
20. S.V. Gajslar, O.I. Semenova, R.G. Sharafutdinov, B.A. Kolesov. Analysis of Raman spectra of amorphous-nanocrystalline silicon films, *Phys. Solid State* **46**, 1528 (2004).
21. G.L. Olson, J.A. Roth. Kinetics of solid phase crystallization in amorphous silicon, *Mater. Sci. Rep.* **3**, 1 (1988).
22. G. Dalba, P. Fornasini, R. Grisenti, F. Rocca, D. Comedi, I. Chambouleyron. Local coordination of Ga impurity in hydrogenated amorphous germanium studied by extended x-ray absorption fine-structure spectroscopy. *Appl. Phys. Lett.* **74**, 281 (1999).
23. Linwei Yu, B. O'Donnell, P.-J. Alet, S. Conesa-Boj, F. Peiró, J. Arbiol, Pere Roca i Cabarrocas. Plasma-enhanced low temperature growth of silicon nanowires and hierarchical structures by using tin and indium catalysts. *Nanotechnology* **20**, 225604 (2009).
24. A. Hiraki. Low temperature reactions at Si/metal interfaces: What is going on at the interfaces? *Surf. Sci. Rep.* **3**, 357 (1984).

25. W. Knaepen, S. Gaudet, C. Detavernier, R.L. Van Meirhaeghe, J.J. Sweet, C. Lavoie. In situ x-ray diffraction study of metal induced crystallization of amorphous germanium. *J. Appl. Phys.* **105**, 083532 (2009).
26. G. Neumann, C. Tuijn. *Self-Diffusion and Impurity Diffusion in Pure Metals: Handbook of Experimental Data* (Elsevier, 2009) [ISBN: 978-1-85617-511-1].
27. S. Sharafat, N. Ghoniem. Summary of thermo-physical properties of sn, and compounds of Sn-H, Sn-O, Sn-C, Sn-Li, and Sn-Si and comparison of properties of Sn, Sn-Li, Li, and Pb-Li. *Report SS/NG: UCLA-UCMEP-00-31* (UCLA, 2000).
28. P. Kringhøj, R.G. Elliman. Diffusion of ion implanted Sn in Si, Si_{1-x}Ge_x, and Ge. *Appl. Phys. Lett.* **65**, 324 (1994).
29. R.P. Thornton, R.G. Elliman, J.S. Williams. Amorphous-to-polycrystalline phase transformations in Sn-implanted silicon. *J. Mater. Res.* **5**, 1003 (1990).
30. G.S. Kulikov, K.Kh. Khodzhaev. Effect of doping with phosphorus on tin diffusion in a-Si: H films. *Fiz. Tekhn. Poluprovodn.* **29**, 961 (1995) (in Russian).
31. S. Coffa, L. Calcagno, S.U. Campisano, G. Calleri, G. Ferla. Diffusion of ion-implanted gold in p-type silicon. *J. Appl. Phys.* **64**, 6291 (1988).
32. J. Hirvonen, A. Anttila. Self-diffusion in silicon as probed by the (p, γ) resonance broadening method. *Appl. Phys. Lett.* **35**, 703 (1979).
33. R.B. Iverson, R. Reif. Recrystallization of amorphized polycrystalline silicon films on SiO₂: Temperature dependence of the crystallization parameters. *J. Appl. Phys.* **62**, 1675 (1987).
34. F. Strauß, L. Dörrer, Th. Geue, J. Stahn, A. Koutsoubas, S. Mattauch, H. Schmidt. Self-diffusion in amorphous silicon. *Phys. Rev. Lett.* **116**, 025901 (2016).
35. U. Köster. Crystallization of amorphous silicon films. *Phys. Stat. Solidi A* **48**, 313 (1978).
36. E. Nygren, A.P. Pogany, K.T. Short, J.S. Williams, R.G. Elliman, J.M. Poate. Impurity-stimulated crystallization and diffusion in amorphous silicon. *Appl. Phys. Lett.* **52**, 439 (1988).
37. E.P. Donovan, F. Spaepen, D. Turnbull, J.M. Poate, D.C. Jacobson. Heat of crystallization and melting point of amorphous silicon. *Appl. Phys. Lett.* **42**, 698 (1983).
38. M.F. Fyhn, J. Chevallier, A.N. Larsen. a-Sn and b-Sn precipitates in annealed epitaxial Si_{0.95}Sn_{0.05}. *Phys. Rev. B* **60**, 5770 (1999).
39. T.H. Yeh, S.M. Hu, R.H. Kastl. Diffusion of tin into silicon. *J. Appl. Phys.* **39**, 4266 (1968).
40. J. Kühnle, R.B. Bergmann, J.H. Werner. Role of critical size of nuclei for liquid-phase epitaxy on polycrystalline Si films. *J. Cryst. Growth* **173**, 62 (1997).
41. R. Sinclair, J. Morgiel, A.S. Kirtikar, I.-W. Wu, A. Chiang. Direct observation of crystallization in silicon by in situ high-resolution electron microscopy. *Ultramicroscopy* **51**, 41 (1993).
42. C.H. Ma, R.A. Swalin. Self diffusion in liquid tin. *J. Chem. Phys.* **36**, 3014 (1962).
43. H. Qinghengt, E.S. Yang, H. Izmirliyan. Diffusivity and growth rate of silicon in solid-phase epitaxy with an aluminum medium. *Solid-State Electron.* **25**, 1187 (1982).

Received 27.09.19.

Translated from Ukrainian by O.I. Voitenko

*Р.М. Руденко, О.О. Войцізовська,
В.В. Войтович, А.Г. Колосюк, М.М. Красько,
В.Ю. Поварчук, М.П. Руденко, Л.М. Кнорозок*

ФОРМУВАННЯ НАНОКРИСТАЛІЧНОГО КРЕМНІЮ В ПЛІВКАХ АМОРФНОГО КРЕМНІЮ, ЛЕГОВАНОГО ОЛОВОМ

Резюме

Досліджено процес формування кристалічної фази кремнію в плівках аморфного кремнію, легovanого оловом. Показано, що включення металевого олова відіграють ключову роль в процесі кристалізації досліджуваних зразків a-SiSn (Sn ~1–10 ат.%) при температурах 300–500 °C. Процес кристалізації умовно можна поділити на два етапи. На першому етапі у об'ємі свіжоосаджених плівок внаслідок дифузії атомів олова в аморфній матриці кремнію відбувається формування металевих включень олова. На другому етапі відбувається формування нанокристалічної фази кремнію внаслідок руху атомів кремнію від аморфної до кристалічної фази через сформовані металеві включення олова. Присутність металевих включень олова забезпечує формування кристалітів кремнію при значно нижчій температурі, ніж температура твердофазної рекристалізації (~750 °C). У роботі проаналізована можливість існування взаємозв'язку між розмірами нанокристалічного кремнію, який формується, та розмірами металевих включень олова, які сприяють його формуванню.